MITSUBISHI ELECTRIC RESEARCH LABORATORIES
https://www.merl.com

Aircraft Approach Management using Reachability and Dynamic Programming

Vinod, Abraham P.; Yamazaki, Sachiyo; Chakrabarty, Ankush; Yoshikawa, Nobuyuki; Di Cairano, Stefano

TR2024-079 June 26, 2024

Abstract

We study the problem of designing safe trajectories for aircraft approach management. Our tractable method designs aircraft trajectories that 1) use only limited admissible maneuvers near the airport, 2) maintains a user-specified separation between aircraft during the entire duration of the approach, and 3) minimizes deviations from user-specified times of arrival at the airport. We use a first-come, first-serve frame- work to design the trajectories for multiple aircraft by solving a collection of single-aircraft trajectory planning problems. We ensure the safety of the overall system by imposing reachability- based constraints on each planning problem. We identify the constraints as well as the trajectories for aircraft using dynamic programming in a three-dimensional space. We validate the efficacy and safety of our method using historical data from Japan's Haneda International Airport.

American Control Conference (ACC) 2024

Mitsubishi Electric Research Laboratories, Inc.
201 Broadway, Cambridge, Massachusetts 02139

Aircraft Approach Management using Reachability and Dynamic Programming

Abraham P. Vinod*, Sachiyo Yamazaki, Ankush Chakrabarty, Nobuyuki Yoshikawa, and Stefano Di Cairano

***Abstract*— We study the problem of designing safe trajectories for aircraft approach management. Our tractable method designs aircraft trajectories that 1) use only limited admissible maneuvers near the airport, 2) maintains a user-specified separation between aircraft during the entire duration of the approach, and 3) minimizes deviations from user-specified times of arrival at the airport. We use a first-come, first-serve framework to design the trajectories for multiple aircraft by solving a collection of single-aircraft trajectory planning problems. We ensure the safety of the overall system by imposing reachability-based constraints on each planning problem. We identify the constraints as well as the trajectories for aircraft using dynamic programming in a three-dimensional space. We validate the efficacy and safety of our method using historical data from Japan's Haneda International Airport.**

I. Introduction

Air traffic is poised to rise back to pre-pandemic levels by the end of 2023 and continue its rapid growth [1]. Given the limited space and congestion with air traffic around existing airports, we need autonomous solutions for safe air traffic management that will help reduce the work load on air traffic controllers, and improve the operating efficiency of the airports. However, these solutions must also be acceptable for pilots and controllers, and compliant with current air traffic control procedures to ensure the possibility of rapid deployment. In this paper, we consider the problem of autonomously designing safe aircraft trajectories during the *approach phase*. The approach phase starts with the aircraft entering the *terminal maneuvering area* (TMA) and ends when the aircraft reaching a *merge point* near the airport. At the merge point, the aircraft initiates a landing pattern, and the aircraft is handed-off to the tower control. Once the aircraft enters a landing traffic pattern, all motion parameters until landing are fixed [2]–[4].

We consider three different maneuvers currently employed for air traffic management near airports — holding pattern (`HOLD`), point merge system (`PMS`), and speed decrement (`DEC`). Each of these maneuvers introduces additional delay in the aircraft's arrival at the merge point. In a `HOLD` maneuver, an aircraft travels in a pre-determined holding pattern. In a `DEC` maneuver, the aircraft reduces its speed while traveling along a straight path. In a `PMS` maneuver, an aircraft flies along a sequencing leg (an arc around the merge point) for a pre-specified duration, after which it heads towards the merge point [4]. To increase the passenger comfort and reduce fuel consumption, we enforce the following preference order when choosing maneuvers for designing aircraft trajectories — `DEC` followed by `PMS` followed by `HOLD`. In this paper, we propose *a dynamic programming-based algorithm to autonomously identify the sequence of maneuvers the pilots of each aircraft must execute, while respecting the desired order of preference, maintaining desired separation between aircraft for safety, and minimizing the deviation of the aircraft's arrival time at the airport from the desired time of arrival*.

Air traffic management has been active area of research for the past several decades [2], [3], [5], [6]. Popular methods to solve air traffic management problems include mixed-integer programming and dynamic programming. Existing mixed-integer programming-based methods for aircraft trajectory generation have mostly focused on `PMS` and/or `HOLD` maneuvers [1], [7]. However, mixed-integer programming-based solutions may not provide real-time guarantees, and therefore may not be practical for busy airports. For real-time updates to approach plans, recent literature also provides practical heuristic solutions, but are limited to `PMS`-only trajectory generation [8]. Dynamic programming-based methods have been typically used for determining landing sequences [5], [9], and not aircraft trajectory generation. Also, it is unclear how these methods can be extended to include `DEC`, while imposing a preference order for the maneuvers.

The main contribution of this paper is a real-time implementable algorithm for designing aircraft trajectories near airport under maneuver, timing, and separation constraints. Our method uses a first-come-first-serve (FCFS) framework to split the air traffic management problem into a collection of single-aircraft scheduling problems, identifies reachability-based constraints on the single-aircraft scheduling problem to ensure safety of the overall system, and then solves the individual single-aircraft scheduling problem using dynamic programming. To enable a tractable grid-based implementation for the dynamic programming, we propose a low-dimensional formulation of the trajectory optimization problem for a single aircraft approaching the airport that incorporates the maneuver constraints. We validate the efficacy and safety of our method using historical data from Japan's Haneda International Airport.

II. Preliminaries

Let $\mathbb{N}_{[a,b]}$ be the set of natural numbers (including a and b) between $a, b \in \mathbb{N}$ with $a \leq b$, and $\|\cdot\|$ denote the Euclidean norm. We use $\langle r, \phi \rangle$ to denote a two-dimensional point in polar coordinates whose distance from origin is $r \geq 0$ and the point has an orientation with respect to `x`-axis as $\phi \in [0, 2\pi)$.

* Corresponding author. Email: `abraham.p.vinod@ieee.org`.
A. Vinod, A. Chakrabarty, and S. Di Cairano are with Mitsubishi Electric Research Laboratories, Cambridge, MA 02139, USA.
S. Yamazaki and N. Yoshikawa are with Mitsubishi Electric Corp., Japan.

A. Reachability of a target tube

We briefly review the concept of reachability of a target tube [10, §4.6]. Consider a nonlinear system,

$$x_{k+1} = f_k(x_k, u_k) \tag{1}$$

with state $x_k \in \mathscr{X} \subseteq \mathbb{R}^n$ and control $u_k \in \mathscr{U} \subset \mathbb{R}^m$. For a horizon $K \in \mathbb{N}$, we wish to identify sets $\{\mathscr{U}_{\text{safe}}(k,x_k)\}_{k=0}^{K-1}$ with $\mathscr{U}_{\text{safe}} \subset \mathscr{U}$ such for an *admissible policy* $\pi = \{\mu_0, \ldots, \mu_{K-1}\}$ with $\mu_k(x_k) \in \mathscr{U}_{\text{safe}}(k,x_k)$, the state of the closed-loop system,

$$x_{k+1} = f_k(x_k, \mu_k(x_k)) \tag{2}$$

belongs to a given (safe) set $\mathscr{S}_{k+1} \subseteq \mathscr{X}$ for $k \in \mathbb{N}_{[-1,K-1]}$. We view the collection of sets $\{\mathscr{S}_k\}_{k=1}^{K}$ as a "tube" within which the state must stay using the available control, and the control problem of interest as the reachability of a target tube, where $\mathscr{S}_k$ is the target set at time k.

We now consider the reachability problem with a target tube $\{\mathscr{S}_k\}_{k=0}^{K}$ where $\mathscr{S}_k \subseteq \mathscr{X} \times \mathscr{U}$ for $k \in \mathbb{N}_{[0,K-1]}$, and $\mathscr{S}_K \subseteq \mathscr{X}$ as a terminal state constraint. For an initial state x_0, we can solve the reachability problem by solving,

$$J^*(x_0) = \min_{\pi \in \Pi} J_\pi(x_0), \tag{3}$$

where

$$J_\pi(x_0) = g_N(x_N) + \sum_{k=0}^{K-1} g_k(x_k, \mu_k(x_k)), \tag{4a}$$

$$g_k(x_k,u_k) = \begin{cases} 0, & (x_k,u_k) \in \mathscr{S}_k, \\ 1, & (x_k,u_k) \notin \mathscr{S}_k, \end{cases} \tag{4b}$$

$$g_K(x_K) = \begin{cases} 0, & x_K \in \mathscr{S}_K, \\ 1, & x_K \notin \mathscr{S}_K, \end{cases} . \tag{4c}$$

In (4a), J_π is the number of violations of the target tube $\{\mathscr{S}_k\}_{k=0}^{K}$ by the closed-loop trajectory corresponding to a policy π. The optimal policy minimizes the number of constraint violations J_π.

We solve (3) using dynamic programming [10]. Specifically, we define a sequence of cost-to-go functions $\{J_k^*\}_{k=0}^{K}$ with $J_K^* \triangleq g_K$, and

$$J_k^*(x_k) = \min_{u_k \in \mathscr{U}(k,x_k)} \left(g_k(x_k,u_k) + J_{k+1}^*(f(x_k,u_k)) \right), \tag{5}$$

for $k \in \mathbb{N}_{[0,K-1]}$. From [10, §4.6], $J^* = J_0^*$, and the set of initial states that solve the reachability problem is given by $\{x_0 : J_0^*(x_0) = 0\}$. Additionally, for each $k \in \mathbb{N}_{[0,K-1]}$,

$$\mathscr{U}_{\text{safe}}(k,x_k) = \left\{ u_k \in \mathscr{U} \,\middle|\, g_k(x_k,u_k) + J_{k+1}^*(f(x_k,u_k)) = 0 \right\}. \tag{6}$$

B. Problem statement

Consider the problem of generating safe trajectories for $N \in \mathbb{N}$ aircraft, where each aircraft $i \in \mathbb{N}_{[1,N]}$ can only perform maneuvers illustrated in Figure 1, which are familiar for pilots, controllers, and air traffic control systems. We focus on the lateral (latitude and longitude) motion of the aircraft for simplicity, and ignore altitude changes. Additionally, we use a polar coordinate system to describe the intermediate points of interest, with the merge point as the origin.

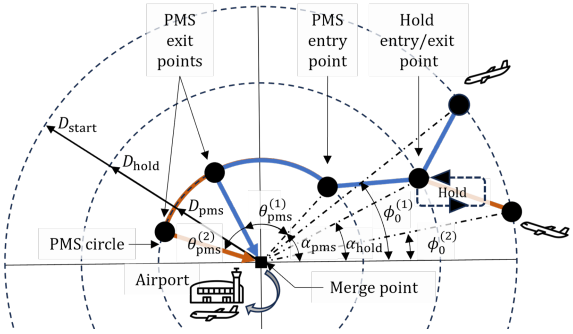

Fig. 1. Typical aircraft trajectories (blue and brown) during the approach phase. The aircraft, upon reaching the merge point, are handed-off to ground control for landing (grey arrow). We are interested in ensuring separation at all times when aircraft are within the PMS circle. The figure illustrates various important waypoints (black).

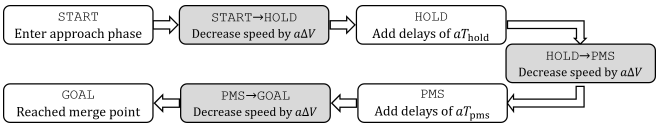

Fig. 2. The aircraft passes through six segments in the approach phase after starting at the START stage. In each segment, the aircraft can perform a specific maneuver $a \in \mathbb{N}$ times.

As illustrated in Figure 2, the aircraft trajectory can be divided into six segments after START — START−HOLD, HOLD, HOLD−PMS, PMS, PMS−GOAL, and GOAL. We use GOAL to indicate that the aircraft reached the merge point.

Initialization: We define the initial stage of the trajectory as START, where the aircraft enters TMA defined as a ball of radius $D_{\text{start}} > 0$ around the merge point. We are provided with the following information about the aircraft at START — the current time $t_0 \geq 0$, the current orientation of the aircraft with respect to the merge point $\phi_0 \in [0, 2\pi)$, and the desired arrival time at the merge point $t_{\text{arrival}} > t_0$. We denote the initial information associated with aircraft $i \in \mathbb{N}_{[1,N]}$ by the tuple $\mathscr{I}_i = \left(t_0^{(i)}, \phi_0^{(i)}, t_{\text{arrival}}^{(i)}\right)$. By design, the position of the aircraft i at START is $\left\langle D_{\text{start}}, \phi_0^{(i)} \right\rangle$. We assume that all aircraft enter the terminal maneuvering area at an identical initial speed V_0, which is reasonable based on standard flightplans and controlled airspace rules.

Speed deceleration maneuver: The aircraft may also be asked to perform speed decrements maneuvers DEC at any or all of the three parts of the trajectory — between START and HOLD entry point, between HOLD exit point and PMS entry point, and between PMS exit point and the merge point. In each of these segments, the aircraft performs an aircraft-independent constant deceleration during a DEC maneuver with the deceleration magnitude $B > 0$. We assume that the aircraft's speed can be reduced in steps of $\Delta V > 0$ by $a\Delta V$ for some $a \in \mathbb{N}_{[0,N_{\text{dec}}]}$ for some $N_{\text{dec}} \in \mathbb{N}$ and a pre-specified speed decrement $\Delta V > 0$.

Holding maneuver: Once the aircraft enters TMA, the aircraft continues towards the HOLD entry point, which is located at $\langle D_{\text{hold}}, \alpha_{\text{hold}} \rangle$ with $D_{\text{hold}} \in (0, D_{\text{start}})$. Upon

reaching the HOLD entry point, the aircraft may be asked to perform $a \in \mathbb{N}_{[0,N_{\text{hold}}]}$ hold maneuvers for some $N_{\text{hold}} \in \mathbb{N}$, or continue towards the merge point. In a HOLD maneuver, the aircraft follows a pre-defined loop that originates and terminates at the HOLD entry point, and each hold maneuver introduces a delay of $T_{\text{hold}} > 0$ minutes.

PMS maneuver: The aircraft continues towards the PMS entry point, which is located at $\langle D_{\text{pms}}, \alpha_{\text{pms}} \rangle$ with $D_{\text{pms}} \in (0, D_{\text{hold}})$. We will refer to the circle centered at the merge point with radius D_{pms} as the PMS circle. Upon reaching the PMS entry point, the aircraft may be asked to continue towards the merge point, or subtend an angle $\theta_{\text{pms}} = a\theta_{\text{pms}}^{\text{step}}$ at the merge point by traveling along the PMS circle at a constant angular rate ω_{pms}. Here, $a \in \mathbb{N}_{[0,N_{\text{pms}}]}$ with $N_{\text{pms}} \triangleq \left\lfloor \Theta_{\text{pms}}^{\max}/\theta_{\text{pms}}^{\text{step}} \right\rfloor$ for some $\Theta_{\text{pms}}^{\max} \in (0, 2\pi)$ and $\theta_{\text{pms}}^{\text{step}} \in (0, \Theta_{\text{pms}}^{\max})$. We will assume $\omega_{\text{pms}} = V_{\text{pms}}/D_{\text{pms}} = (V_0 - \vartheta_m \Delta V)/D_{\text{pms}}$, where V_{pms} denotes the speed of the aircraft at the PMS entry point that may be computed using ϑ_m, the number of velocity decrements requested during the maneuvers START–HOLD and HOLD–PMS. A PMS maneuver delays the aircraft by aT_{pms}, where $T_{\text{pms}} \triangleq (D_{\text{pms}}\theta_{\text{pms}}^{\text{step}})/(V_0 - \vartheta_m \Delta V)$. Upon exiting the PMS circle, the aircraft heads towards the merge point.

Trajectory optimization problem: We design aircraft trajectories to optimize the following problem:

- Performance objective: The aircraft must minimize deviation (if any) from its desired arrival time.
- Maneuver constraints: The aircraft motion is subject to constraints imposed by the maneuvers. Also, we prefer DEC maneuvers over PMS maneuvers, and PMS maneuvers over HOLD maneuvers, when possible.
- Information constraint: We have the initial information of aircraft $\mathscr{I}_i$, only when the aircraft i enters TMA.
- Safety constraint: For safety, the aircraft must maintain a separation of $D_{\text{sep}} > 0$ between any other aircraft, when the both aircraft are at least D_{pms}-close to the merge point (not farther than D_{pms}).

We use the information constraint to account for the limitations of the radars employed by typical airports as well as to accommodate any unexpected delays faced by an aircraft during its journey. We restrict the safety constraint to aircraft that are within or on the PMS circle for simplicity.

Problem 1. *Design an algorithm to construct aircraft trajectories comprised only of the admissible maneuvers (DEC, PMS, and HOLD, in their order of preference), such that each aircraft's trajectory minimizes the performance objective while satisfying constraints arising from maneuver, information, and safety/separation constraints.*

Due to the information constraint and to ensure tractability, we formulate a FCFS-based algorithm to solve Problem 1. FCFS-based algorithms are popular in air traffic management as they are easy to implement and they reduce pilot workload by not modifying the operating instructions once relayed [1]–[3], [6]. However, FCFS-based algorithms can be suboptimal for airport throughput. To optimize throughput, *constrained position switching*-based algorithms may be used, which allows limited changes to relayed instructions [9].

III. Trajectory optimization for single aircraft

In this section, we formulate the single aircraft trajectory optimization problem as a low-dimensional Markov Decision Process (MDP). The proposed formulation enforces the maneuver constraints by design, and we choose a reward function motivated by the performance objective as well as the maneuver preferences.

We cast the problem of trajectory optimization for a single aircraft as a discrete-time, mixed-state MDP with discrete action space. Denoting the six segments after START (see Fig. 2) of the aircraft trajectory using $m \in \mathbb{N}_{[0,5]}$, the aircraft trajectory design starts with the aircraft in START–HOLD segment $m = 0$, and terminates at the GOAL segment $m = 5$. Therefore, we use m analogous to "time" to define the MDP.

State space: The state $x \in \mathscr{X} \triangleq \mathbb{R} \times [0, 2\pi) \times \mathbb{N}_{[0,3N_{\text{dec}}]}$ at stage m is given by the triplet

$$x_m = (\Delta t_m, \phi_m, \vartheta_m), \tag{7}$$

where $\Delta t_m \triangleq t_m - t_{\text{arrival}}$ with $t_m \in \mathbb{R}$ denoting the time an aircraft enters segment m, ϕ_m denotes the orientation of the aircraft with respect to the merge point at the start of the segment m, and ϑ_m denotes the number of executed speed decrements prior to the segment m. By construction, the speed of the aircraft at the start of segment m is given by

$$V_m = V_0 - \vartheta_m \Delta V, \tag{8}$$

and the initial state of the MDP is $x_0 = (t_0 - t_{\text{arrival}}, \phi_0, 0)$.

Action space: At each segment $m \in \mathbb{N}_{[0,5]}$, we can apply a discrete action $a \in \mathscr{A}(m) \subset \mathbb{N}$. Specifically,

$$\mathscr{A}(m) = \begin{cases} \mathbb{N}_{[0,N_{\text{hold}}]}, & m = 1 \ (\texttt{HOLD}), \\ \mathbb{N}_{[0,N_{\text{pms}}]}, & m = 3 \ (\texttt{PMS}), \\ \emptyset, & m = 5 \ (\texttt{GOAL}), \\ \mathbb{N}_{[0,N_{\text{dec}}]}, & \text{otherwise.} \end{cases} \tag{9}$$

Transition function: We model the aircraft's motion during the approach as a point mass constrained to the path described in Figure 1.

For DEC maneuver ($m \in \{0, 2, 4\}$), the next state under a speed decrement action $a \in \mathscr{A}(m) = \mathbb{N}_{[0,N_{\text{dec}}]}$ is $x_{m+1} = (\Delta t_{m+1}, \vartheta_{m+1}, \phi_{m+1})$, where

$$\Delta t_{m+1} = \Delta t_m + \frac{2BD_{\text{gap}}^{(m)} - (a\Delta V)^2}{2B(V_0 - (\vartheta_m + a)\Delta V)}, \tag{10a}$$

$$\phi_{m+1} = \begin{cases} \alpha_{\text{hold}}, & m = 0, \\ \alpha_{\text{pms}}, & m = 2, \\ \phi_m, & m = 4, \end{cases} \tag{10b}$$

$$\vartheta_{m+1} = \vartheta_m + a, \tag{10c}$$

where $D_{\text{gap}}^{(m)}$ is the distance between the current position and the entry point of the next segment. Specifically,

$$D_{\text{gap}}^{(m)} = \begin{cases} \| \langle D_{\text{start}}, \phi_0 \rangle - \langle D_{\text{hold}}, \alpha_{\text{hold}} \rangle \|, & m = 0, \\ \| \langle D_{\text{hold}}, \alpha_{\text{hold}} \rangle - \langle D_{\text{pms}}, \alpha_{\text{pms}} \rangle \|, & m = 2, \\ D_{\text{pms}}, & m = 4. \end{cases} \tag{11}$$

See Appendix A for the derivation of (10a).

For HOLD ($m=1$) and PMS ($m=3$) maneuvers, the next state under action $a \in \mathscr{A}(1) = \mathbb{N}_{[0,N_{\text{hold}}]}$ and $a \in \mathscr{A}(3) = \mathbb{N}_{[0,N_{\text{pms}}]}$ are $x_{m+1} = (\Delta t_{m+1}, \vartheta_{m+1}, \phi_{m+1})$ respectively, with

$$\Delta t_{m+1} = \begin{cases} \Delta t_m + aT_{\text{hold}} & m=1, \\ \Delta t_m + aT_{\text{pms}} & m=3, \end{cases} \tag{12a}$$

$$\phi_{m+1} = \begin{cases} \alpha_{\text{hold}}, & m=1, \\ \alpha_{\text{pms}} + a\theta^{\text{step}}_{\text{pms}}, & m=3, \end{cases} \tag{12b}$$

$$\vartheta^+ = \vartheta. \tag{12c}$$

Reward function: We define the reward function as follows,

$$r(s,a) = \begin{cases} \text{TerminalReward}(\Delta t_5) & m=5, \\ -\text{ActionPenalty}(m)a, & \text{otherwise}, \end{cases} \tag{13}$$

where $\text{TerminalReward} : \mathbb{R} \to \mathbb{R}$ is a terminal reward function on Δt_5, and $\text{ActionPenalty} : \mathbb{N}_{[0,4]} \to \mathbb{R}$ penalizes actions and enforces the preference order for the maneuvers. Specifically, TerminalReward is a continuous function that rewards minimal deviation of Δt_5 from zero and decays with increasing deviation from zero, i.e., we get the maximum reward when the aircraft i reaches the airport at $t^{(i)}_{\text{arrival}}$. On the other hand, ActionPenalty enforces the order of preference with $\text{ActionPenalty}(0) = \text{ActionPenalty}(2) = \text{ActionPenalty}(4) < \text{ActionPenalty}(3) < \text{ActionPenalty}(1)$.

Since MDP has a low-dimensional state-space and a single-dimensional discrete action space, we can leverage dynamic programming to design an optimal single-aircraft trajectory. Specifically, we set up value functions $\mathscr{V}^*_m : \mathscr{X} \to \mathbb{R}$ for $m \in \mathbb{N}_{[0,5]}$ defined by the recursion,

$$\mathscr{V}^*_5(\Delta t_m, \cdot, \cdot) = \text{TerminalReward}(\Delta t), \tag{14a}$$

$$\mathscr{V}^*_m(x_m) = \max_{a \in \mathscr{A}(m)} \left(r(x_m, a) + \mathscr{V}^*_{m+1}(x_{m+1}) \right), \tag{14b}$$

for $m \in \mathbb{N}_{[0,4]}$. Given value functions $\{\mathscr{V}^*_m\}_{m \in \mathbb{N}_{[0,5]}}$, we can identify the optimal action at any state x by,

$$a^* = \arg\max_{a \in \mathscr{A}(m)} \left(r(x_m, a) + \mathscr{V}^*_{m+1}(x_{m+1}) \right). \tag{15}$$

Equations (14) and (15) enable the design of trajectories for single aircraft, and incorporate the performance objective and maneuver constraints in Section II-B. In a practical implementation, we define a grid over $\mathscr{X}$ and perform the backward recursion described in (14) to obtain an approximation of the value functions $\{\widehat{\mathscr{V}_m}\}_{m \in \mathbb{N}_{[0,5]}}$.

IV. Safe trajectory optimization for multiple aircraft

In this section, we propose a FCFS framework that solves Problem 1, by solving a collection of single aircraft trajectory optimization problems under additional constraints in the action space. Under FCFS framework, during the design of the trajectory for aircraft $i \in \mathbb{N}_{[2,N]}$, we know the trajectory of aircraft $j \in \mathbb{N}_{[1,i-1]}$. Consequently, we can use the reachability of target tube reviewed in Section II-A to identify the set of admissible waypoints and actions for aircraft i that do not violate the separation constraint. The reachability analysis characterizes a restricted *safe* action space $\mathscr{A}_{\text{safe}}$ that ensures safety (see (6)). Thus, by replacing $\mathscr{A}$ in (14) and (15) with $\mathscr{A}_{\text{safe}}$, we can enforce the safety constraint involving multiple aircraft in the single aircraft trajectory optimization, and solve Problem 1.

TABLE I

Stage costs for $\mathscr{A}_{\text{safe}}$ computation for safe trajectory optimization for multiple aircraft based on Section II-A

g	Indicator function	Equation numbers
g_5	$I_{(5,)}$	(38)
g_4	$\max(I_{(4,3)}, I_{(4,4)}, I_{(4,5)})$	(34), (21), (39)
g_3	$\max(I_{(3,3)}, I_{(3,4)})$	(26), (37)
g_0, g_1, g_2	0	-

For the state $x^{(i)}_m \in \mathscr{X}$ defined in (7) and the input (action) $a^{(i)}_m \in \mathscr{A}(m)$ defined in (9), the nonlinear dynamics $f_m : \mathscr{X} \times \mathscr{A}(m) \to \mathscr{X}$ in (1) are characterized by (10) and (12).

Next, we complete the definition of the reachability problem (3) by identifying the indicator functions $g_m : \mathscr{X} \times \mathscr{A}(m) \to \{0,1\}$ that characterizes safe state-actions pairs $(x^{(i)}_m, a^{(i)}_m)$ for each $m \in \mathbb{N}_{[0,4]}$, such that no collision occurs at all time between the segments m and $m+1$ between the aircraft i and an aircraft $j \in \mathbb{N}_{[1,i-1]}$.

Table I list the definitions of g_m using $I_{(m_i,m_j)}$, where $I_{(m_i,m_j)}$ are defined by considering state-action pairs $(x^{(i)}_{m_i}, a^{(i)}_{m_i})$ that result in collision when aircraft i and j are segments m_i and m_j respectively. The use of 'max' in the definition of g_m ensures that $g_m = 1$ if any of the associated indicator functions evaluates to one (i.e. a constraint is violated).

We now briefly discuss the derivations for $I_{(m_i,m_j)}$. From Figure 1, we must consider five different scenarios.

1) Both aircraft have $m=4$: In this scenario, both aircraft are between PMS exit point and the merge point (see Figure 3.a), and can perform speed decrements. Specifically, each aircraft $k \in \{i,j\}$ undergoes a DEC maneuver of $a^{(k)}_4$ speed decrements respectively. Then, each aircraft proceeds to the merge point with a constant speed.

This particular scenario occurs for $\tau \in \mathscr{T}^{(i,j)}_{(4,4)}$, with

$$\mathscr{T}^{(i,j)}_{(4,4)} \triangleq \bigcap_{k \in \{i,j\}} [t^{(k)}_4, t^{(k)}_5] = \left[\max_{k \in \{i,j\}} \left(t^{(k)}_4 \right), \min_{k \in \{i,j\}} \left(t^{(k)}_5 \right) \right]. \tag{16}$$

The safety constraint in this scenario is,

$$\left\| \left\langle r^{(i)}(\tau), \phi^{(i)}(\tau) \right\rangle - \left\langle r^{(j)}(\tau), \phi^{(j)}(\tau) \right\rangle \right\| \geq D_{\text{sep}}, \tag{17}$$

for all $\tau \in \mathscr{T}^{(i,j)}_{(4,4)}$. From the triangle inequality (Figure 3.a),

$$\min_{\tau \in \mathscr{T}^{(i,j)}_{(4,4)}} |r^{(i)}(\tau) - r^{(j)}(\tau)| \geq D_{\text{sep}} \Longrightarrow (17). \tag{18}$$

By equations of motion, we have

$$r^{(k)}(\tau) = \begin{cases} D_{\text{pms}} - V^{(k)}_4 \left(\tau - t^{(k)}_4 \right) + \frac{B}{2} \left(\tau - t^{(k)}_4 \right)^2, & t^{(k)}_4 \leq \tau \leq t^{(k)}_{4,\text{int}}, \\ D_{\text{pms}} - D^{(k)}_{\text{dec}} - V^{(k)}_5 \left(\tau - \left(t^{(k)}_4 + \frac{a^{(k)} \Delta V}{B} \right) \right), & t^{(k)}_{4,\text{int}} < \tau \leq t^{(k)}_5, \end{cases} \tag{19}$$

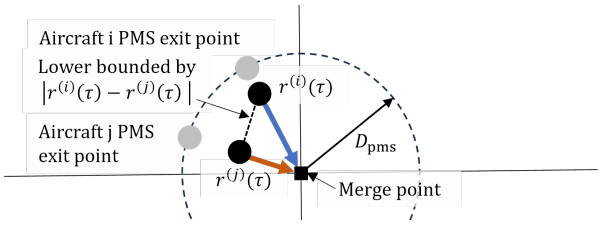

a) Both aircraft have $m = 4$, where the lower bound on LHS of (17) is from triangle inequality ($c \geq |a-b|$ for any triangle with sides a, b, and c).

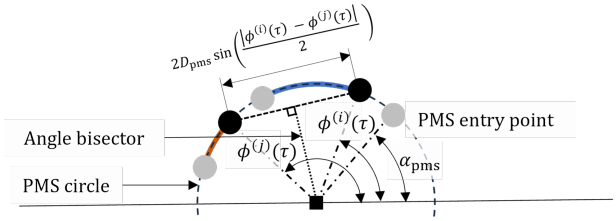

b) Both aircraft have $m = 3$, where the aircraft separation can be expressed exactly using the difference between $\phi^{(i)}(\tau)$ and $\phi^{(j)}(\tau)$.

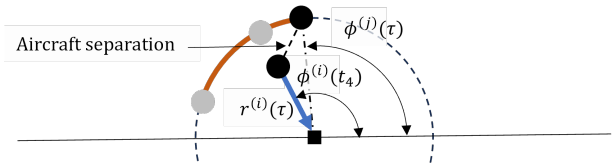

c) Aircraft i has $m = 4$ and aircraft j has $m = 3$, where the aircraft separation is analyzed using the parallelogram law.

Fig. 3. Various scenarios considered for the safety constraint.

with $t_{4,\text{int}}^{(k)} = t_4^{(k)} + \frac{a^{(k)}\Delta V}{B}$ since each aircraft k decelerates for a duration of $(a^{(k)}\Delta V)/B$, $V_m^{(k)}$ given by (8), and $D_{\text{dec}}^{(k)}$ denoting the distance traveled by aircraft k,

$$D_{\text{dec}}^{(k)} = \frac{\left(V_4^{(k)}\right)^2 - \left(V_5^{(k)}\right)^2}{2B}. \tag{20}$$

We encode the safety condition in (18) for aircraft $i \in \mathbb{N}_{[2,N]}$ using an indicator function $I_{(4,4)} : \mathscr{X} \times \mathscr{A}(4) \to \{0,1\}$,

$$I_{(4,4)}\left(x_4^{(i)}, a_4^{(i)}\right) = \begin{cases} 0, & \min\limits_{j \in \mathbb{N}_{[1,i-1]}} \min\limits_{\tau \in \mathscr{T}_{(4,4)}^{(i,j)}} |r^{(i)}(\tau) - r^{(j)}(\tau)| \geq D_{\text{sep}}, \\ 1, & \text{otherwise.} \end{cases} \tag{21}$$

2) Both aircraft have $m = 3$: In this scenario, both aircraft are on PMS segment (Figure 3.b). Specifically, each aircraft $k \in \{i, j\}$ travels along the PMS circle, subtending an angle of $\theta_{\text{pms}}^{(k)} = a_3^{(k)} \theta_{\text{pms}}^{\text{step}}$ at a constant rate $\omega_{\text{pms}}^{(k)} = \frac{V_0 - \vartheta_3 \Delta V}{D_{\text{pms}}}$ during the PMS maneuver.

This particular scenario occurs for $\tau \in \mathscr{T}_{(3,3)}^{(i,j)}$, with

$$\mathscr{T}_{(3,3)}^{(i,j)} \triangleq \bigcap_{k \in \{i,j\}} [t_3^{(k)}, t_4^{(k)}] = \left[\max_{k \in \{i,j\}} \left(t_3^{(k)}\right), \min_{k \in \{i,j\}} \left(t_4^{(k)}\right)\right]. \tag{22}$$

We define $\phi^{(k)}(\tau)$ as the orientation of aircraft $k \in \{i, j\}$ with respect to the merge point at $\tau \in \mathscr{T}_{(3,3)}^{(i,j)}$, with

$$\phi^{(k)}(\tau) = \alpha_{\text{pms}} + \omega_{\text{pms}}^{(k)} \left(\tau - t_3^{(k)}\right). \tag{23}$$

By design, $\phi^{(k)}\left(t_3^{(k)}\right) = \alpha_{\text{pms}}$ and $\phi^{(k)}\left(t_4^{(k)}\right) = \alpha_{\text{pms}} + \theta_{\text{pms}}^{(k)}$.

The safety constraint in this scenario is,

$$\left\| \left\langle D_{\text{pms}}, \phi^{(i)}(\tau) \right\rangle - \left\langle D_{\text{pms}}, \phi^{(j)}(\tau) \right\rangle \right\| \geq D_{\text{sep}}, \tag{24}$$

for all $\tau \in \mathscr{T}_{(3,3)}^{(i,j)}$. Since the bisector of the angle subtended by the arc connecting $\left\langle D_{\text{pms}}, \phi^{(i)}(\tau) \right\rangle$ and $\left\langle D_{\text{pms}}, \phi^{(j)}(\tau) \right\rangle$ at the merge point is also a perpendicular bisector of the line joining them (see Figure 3.b), LHS of (24) can be simplified,

$$\left\| \left\langle D_{\text{pms}}, \phi^{(i)}(\tau) \right\rangle - \left\langle D_{\text{pms}}, \phi^{(j)}(\tau) \right\rangle \right\| = 2D_{\text{pms}} \sin\left(\frac{|\phi^{(i)}(\tau) - \phi^{(j)}(\tau)|}{2}\right).$$

Consequently, we can reformulate (24) as

$$\min_{\tau \in \mathscr{T}_{(3,3)}^{(i,j)}} |\phi^{(i)}(\tau) - \phi^{(j)}(\tau)| \geq \Phi_{(3,3)}^{(i,j)} \triangleq 2\sin^{-1}\left(\frac{D_{\text{sep}}}{2D_{\text{pms}}}\right) \iff (24). \tag{25}$$

Similarly to (21), we encode (25) for aircraft $i \in \mathbb{N}_{[2,N]}$ using an indicator function $I_{(3,3)} : \mathscr{X} \times \mathscr{A}(3) \to \{0,1\}$,

$$I_{(3,3)}\left(x_3^{(i)}, a_3^{(i)}\right) = \begin{cases} 0, & \min\limits_{j \in \mathbb{N}_{[1,i-1]}} \min\limits_{\tau \in \mathscr{T}_{(3,3)}^{(i,j)}} |\phi^{(i)}(\tau) - \phi^{(j)}(\tau)| \geq \Phi_{(3,3)}^{(i,j)}, \\ 1, & \text{otherwise.} \end{cases} \tag{26}$$

3) Aircraft i has $m = 4$, aircraft $j \in \mathbb{N}_{[1,i-1]}$ has $m = 3$: In this scenario, aircraft i is between PMS exit point and GOAL (see Figure 3.c), while aircraft j is on PMS segment.

This particular scenario occurs for $\tau \in \mathscr{T}_{(4,3)}^{(i,j)}$, with

$$\mathscr{T}_{(4,3)}^{(i,j)} \triangleq \left[t_4^{(i)}, t_5^{(i)}\right] \bigcap \left[t_3^{(j)}, t_4^{(j)}\right], \tag{27}$$

and the safety constraint in this scenario is,

$$\left\| \left\langle r^{(i)}(\tau), \phi_4^{(i)} \right\rangle - \left\langle D_{\text{pms}}, \phi^{(j)}(\tau) \right\rangle \right\| \geq D_{\text{sep}}, \tag{28}$$

for all $\tau \in \mathscr{T}_{(4,3)}^{(i,j)}$. By parallelogram law, the LHS of (28) is

$$\begin{aligned} &\left\| \left\langle r^{(i)}(\tau), \phi_4^{(i)} \right\rangle - \left\langle D_{\text{pms}}, \phi^{(j)}(\tau) \right\rangle \right\|^2 \\ &= \left(D_{\text{pms}} - r^{(i)}(\tau)\right)^2 + 2D_{\text{pms}} r^{(i)}(\tau) \left(1 - \cos\left(\phi_4^{(i)} - \phi^{(j)}(\tau)\right)\right), \end{aligned} \tag{29}$$

Thus, we have two disjoint sufficient conditions for (28):

$$D_{\text{pms}} - r^{(i)}(\tau) \geq D_{\text{sep}}, \text{ OR} \tag{30a}$$

$$D_{\text{pms}} - r^{(i)}(\tau) < D_{\text{sep}} \text{ and } \cos\left(\phi_4^{(i)} - \phi^{(j)}(\tau)\right) \leq c_{\text{thresh}}, \tag{30b}$$

where

$$c_{\text{thresh}} = 1 - \frac{D_{\text{sep}}^2}{2D_{\text{pms}}(D_{\text{pms}} - D_{\text{sep}})}. \tag{31}$$

Here, we have (30a) by requiring that the first term in (29) to be at least D_{sep}^2 and observing that the second term in (29) is nonnegative. On the other hand, we have (30b) by requiring that the second term in (29) to be at least D_{sep}^2.

Define $t_{\text{create-sep}}^{(i)} > 0$ such that $r^{(i)}\left(t_4^{(i)} + t_{\text{create-sep}}^{(i)}\right) = D_{\text{pms}} - D_{\text{sep}}$. We can compute $t_{\text{create-sep}}^{(i)}$ by solving either a linear or a quadratic equation (see (19)). Since $r^{(i)}$ is

a decreasing function in τ, (30a) is trivially satisfied for $\tau \in \left[t_4^{(i)} + t_{\text{create-sep}}^{(i)}, t_5^{(i)}\right]$. Thus, from (30b),

$$\min_{\tau \in \mathscr{T}_{(4,3)}^{(i,j)}} \left| \phi_4^{(i)} - \phi^{(j)}(\tau) \right| \geq \Phi_{(4,3)}^{(i,j)} \triangleq \cos^{-1}(c_{\text{thresh}}) \Longrightarrow (28), \quad (32)$$

with

$$\widehat{\mathscr{T}}_{(4,3)}^{(i,j)} = \left[t_4^{(i)}, t_4^{(i)} + t_{\text{create-sep}}^{(i)}\right] \bigcap \left[t_3^{(j)}, t_4^{(j)}\right] \subset \mathscr{T}_{(4,3)}^{(i,j)}. \quad (33)$$

We encode the safety condition in (32) for aircraft $i \in \mathbb{N}_{[2,N]}$ using an indicator function $I_{(4,3)} : \mathscr{X} \times \mathscr{A}(4) \to \{0,1\}$,

$$I_{(4,3)}\left(x_4^{(i)}, a_4^{(i)}\right) = \begin{cases} 0, & \min\limits_{j \in \mathbb{N}_{[1,i-1]}} \min\limits_{\tau \in \widehat{\mathscr{T}}_{(4,3)}^{(i,j)}} \left| \phi_4^{(i)} - \phi^{(j)}(\tau) \right| \geq \Phi_{(4,3)}^{(i,j)}, \\ 1, & \text{otherwise.} \end{cases} \quad (34)$$

Here, $I_{(4,3)}$ depends on $\left(x_4^{(i)}, a_4^{(i)}\right)$, since we require $\phi_4^{(i)}$ in (30), and Δt_4, ϑ_4, $a_4^{(i)}$ for the computation of $t_{\text{create-sep}}^{(i)}$ (and thereby, $\widehat{\mathscr{T}}_{(4,3)}^{(i,j)}$).

4) Aircraft i has $m = 3$, aircraft $j \in \mathbb{N}_{[1,i-1]}$ has $m = 4$: In this scenario, aircraft i is on PMS segment, while aircraft j is between PMS exit point and GOAL. By arguments used to derive (32), a sufficient condition for safety is,

$$\min_{\tau \in \mathscr{T}_{(3,4)}^{(i,j)}} \left| \phi^{(i)}(\tau) - \phi_4^{(j)} \right| \geq \Phi_{(3,4)}^{(i,j)} = \Phi_{(4,3)}^{(i,j)}, \quad (35)$$

with

$$\widehat{\mathscr{T}}_{(3,4)}^{(i,j)} = \left[t_3^{(i)}, t_4^{(i)}\right] \bigcap \left[t_4^{(j)}, t_4^{(j)} + t_{\text{create-sep}}^{(j)}\right], \quad (36)$$

where $t_{\text{create-sep}}^{(j)} > 0$ is such that $r^{(j)}\left(t_4^{(j)} + t_{\text{create-sep}}^{(j)}\right) = D_{\text{pms}} - D_{\text{sep}}$.

Similarly to (34), we encode (35) for aircraft $i \in \mathbb{N}_{[2,N]}$ using an indicator function $I_{(3,4)} : \mathscr{X} \times \mathscr{A}(3) \to \{0,1\}$,

$$I_{(3,4)}\left(x_3^{(i)}, a_3^{(i)}\right) = \begin{cases} 0, & \min\limits_{j \in \mathbb{N}_{[1,i-1]}} \min\limits_{\tau \in \widehat{\mathscr{T}}_{(3,4)}^{(i,j)}} \left| \phi^{(i)}(\tau) - \phi_4^{(j)} \right| \geq \Phi_{(3,4)}^{(i,j)}, \\ 1, & \text{otherwise.} \end{cases} \quad (37)$$

Here, $I_{(3,4)}$ depends on $\left(x_3^{(i)}, a_3^{(i)}\right)$, since we require Δt_3 and ϑ_4 for the computation of $\phi^{(i)}$ (see (23)), and $a_3^{(i)}$ to determine $t_4^{(i)}$ (and thereby, $\widehat{\mathscr{T}}_{(3,4)}^{(i,j)}$).

5) At least one aircraft has $m = 5$: This scenario considers the case where one of the aircraft has been handed-off to tower control for landing. For the case where aircraft $i \in \mathbb{N}_{[2,N]}$ has $m = 5$, we require the separation between the preceding and succeeding aircraft reaching the merge point to maintain some pre-specified time separation $T_{\text{sep}} > 0$. Thus, we define an indicator function $I_{(5,)} : \mathscr{X} \to \{0,1\}$,

$$I_{(5,)}\left(x_5^{(i)}\right) = \begin{cases} 0, & \min_{j \in \mathbb{N}_{[1,i-1]}} \left| t_5^{(j)} - t_5^{(i)} \right| \geq T_{\text{sep}}, \\ 1, & \text{otherwise.} \end{cases} \quad (38)$$

Algorithm 1: Safe trajectory generation for aircraft i

Input: Aircraft information $\{\mathscr{I}_j\}_{j=1}^{i}$, approach parameters $(D_{\text{start}}, D_{\text{hold}}, D_{\text{pms}}, \alpha_{\text{hold}}, \alpha_{\text{pms}}, N_{\text{hold}}, T_{\text{hold}}, N_{\text{pms}}, \theta_{\text{pms}}^{\text{step}}, \Delta V, N_{\text{dec}}, B, D_{\text{sep}}, T_{\text{sep}})$, grid Δt_{grid}, ϕ_{grid}, state-action pairs $\{(x_m^{(j)}, a_m^{(j)})\}_{m=0}^{4}$ and $x_5^{(j)}$ of aircraft $j \in \mathbb{N}_{[1,i-1]}$ $(i \geq 2)$

Output: State-action pairs $\{(x_m^{(i)}, \widehat{a}_m^{(i)})\}_{m=0}^{4}$ and $x_5^{(i)}$ for aircraft i, that together characterizes its trajectory

1: Compute $\{\widehat{J}_m\}_{m=0}^{5}$ using (5) and Table I
2: Compute $\{\widehat{\mathscr{A}_{\text{safe}}}(m)\}_{m=0}^{5}$ using (6), where $J^* \rightrightarrows \widehat{J}$
3: Compute $\{\widehat{\mathscr{V}}_m\}_{m=0}^{5}$ using (14), where $\mathscr{A} \rightrightarrows \widehat{\mathscr{A}_{\text{safe}}}$
4: Compute $\widehat{a}$ using (15), where $\mathscr{A} \rightrightarrows \widehat{\mathscr{A}_{\text{safe}}}$ and $\mathscr{V}^* \rightrightarrows \widehat{\mathscr{V}}$

On the other hand, to enforce the time separation constraint for aircraft $i \in \mathbb{N}_{[2,N]}$ has $m = 4$, we define an indicator function $I_{(4,5)} : \mathscr{X} \times \mathscr{A}(4) \to \{0,1\}$,

$$I_{(4,5)}\left(x_4^{(i)}, a_4^{(i)}\right) = \begin{cases} 0, & \min_{j \in \mathbb{N}_{[1,i-1]}} \left| t_4^{+,(i)} - t_5^{(j)} \right| \geq T_{\text{sep}}, \\ 1, & \text{otherwise,} \end{cases} \quad (39)$$

where $t_4^{+,(i)} = t_5^{(i)}$ corresponding to $\left(x_4^{(i)}, a_4^{(i)}\right)$.

We ignore the rest of the scenarios, since they have at least one aircraft with $m \leq 2$. In other words, one of the aircraft is farther from the merge point by D_{pms}, and no separation constraint needs to be imposed.

Remark 1 (IMPLEMENTATION OF $I_{(m_i,m_j)}$)**.** *First, recall that the global minimum of an optimization over an empty interval is $+\infty$ (optimization is infeasible). Consequently, as an example, $I_{(4,4)}\left(x_4^{(i)}, a_4^{(i)}\right) = 0$ for any $(x_4^{(i)}, a_4^{(i)})$, when $\mathscr{T}_{(4,4)}^{(i,j)} = \emptyset$. Second, most of the indicator functions $I_{(m_i,m_j)}$ defined in this section requires the computation of the global minimum of a collection of one-dimensional functions over an interval, where each function is a composition of $|\cdot|$ and a quadratic/linear function. Using simple arguments from calculus, we can solve these global optimization problems without requiring solvers.*

A. Summarizing the proposed method

We summarize the proposed method, which solves Problem 1, in Algorithm 1. For each new aircraft i, Algorithm 1 solves two dynamic programming problems.

Since each dynamic programming problem involves a three-dimensional state space (two dimensions are continuous and one dimension is discrete) and a one-dimensional, discrete action space, we can approximate the dynamic programming recursions via a grid. We denote the approximations using $\widehat{(\cdot)}$, and use $\rightrightarrows$ to denote replacements of functions/sets with their grid-based approximations.

V. SIMULATIONS WITH DATA FROM HANEDA AIRPORT

We validated our method in numerical simulations using historical data from the Haneda International Airport. We collected aircraft names as well as their scheduled arrival times for 30 aircraft from [11]. We chose $D_{\text{start}} = 100$ nm (nautical miles), $D_{\text{hold}} = 60$, $D_{\text{pms}} = 45$, $\alpha_{\text{hold}} = \alpha_{\text{pms}} = -75^\circ$,

TABLE II

SUMMARY OF THE NUMERICAL VALIDATION USING 4-HOUR DATA FROM HANEDA INTERNATIONAL AIRPORT WITH 30 AIRCRAFT. WE REPORT (0.05,0.5,0.95)-QUANTILES FOR THE UTILIZATION.

Property	Quantity
Number of safety violations	0
Aircraft that reach within 1 min. of t_{arrival}	66.67%
Aircraft that reach within 2 min. of t_{arrival}	99.03%
Utilization of DEC	83.3% / 93.3% / 96.6%
Utilization of PMS	66.6% / 73.3% / 93.3%
Utilization of HOLD	13.3% / 23.3% / 33.3%

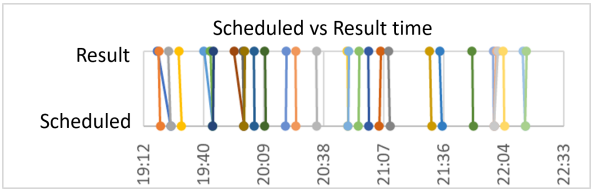

Fig. 4. Arrival schedule and result

$N_{\text{hold}} = 5$, $T_{\text{hold}} = 3$ min., $N_{\text{pms}} = 150$, $\theta_{\text{pms}}^{\text{step}} = 1^\circ$, $\Delta V = 10$ knots, $N_{\text{dec}} = 5$, $D_{\text{sep}} = 2.5$ nm, and $T_{\text{sep}} = 1$ min. We chose ϕ_{grid} as a uniform grid in $[0, 2\pi)$ in step sizes of $\pi/180$, and Δt_{grid} as a grid over five hours in step sizes of 10 seconds. We assumed that the aircraft reached TMA 1 hour before the scheduled arrival time, chose ARLON (a fix near Haneda Airport) as the merge point, and set up appropriate entry points for HOLD and PMS maneuvers.

Table II summarizes various performance and safety metrics associated with the method. As desired, no collisions occurred during the simulation. Additionally, the utilization quantiles show that the trajectories following the desired preference order. Note that the computation time per aircraft was less than 200 s on a standard desktop computer, running non-optimized Python code.

Figure 4 shows the arrival schedule. As expected, the proposed method spreads out the arrival schedule and spaces out the trajectories to avoid collisions, while minimizing deviations.

VI. CONCLUSION

We propose a tractable method using reachability and dynamic programming to design aircraft trajectories for safe air traffic management. Our FCFS-based method utilizes a low-dimensional formulation of the single aircraft trajectory optimization problem, and characterizes the system-level safety constraints as constraints in the available actions for the single aircraft at each segment.

Our future work will investigate the use of constrained position switching to optimize airport throughput, and consider more realistic aircraft dynamics.

REFERENCES

[1] S. Lee, Y. Hong, and Y. Kim, "Optimal scheduling algorithm in point merge system including holding pattern based on MILP," in *7th European Conference for Aeronautics and Aerospace Sciences (EUCASS), Milan, Italy*, 2017.

[2] S. Ikli, C. Mancel, M. Mongeau, X. Olive, and E. Rachelson, "The aircraft runway scheduling problem: A survey," *Computers & Operations Research*, vol. 132, p. 105336, 2021.

[3] J. A. Bennell, M. Mesgarpour, and C. N. Potts, "Airport runway scheduling," *4OR*, vol. 9, pp. 115–138, 2011.

[4] EUROCONTROL, "Point merge system," (Available online) https://www.eurocontrol.int/concept/point-merge.

[5] H. N. Psaraftis, "A dynamic programming approach for sequencing groups of identical jobs," *Operations Research*, vol. 28, no. 6, pp. 1347–1359, 1980.

[6] D. Gui, M. Le, Z. Huang, J. Zhang, and A. D'Ariano, "Optimal aircraft arrival scheduling with continuous descent operations in busy terminal maneuvering areas," *Journal of Air Transport Management*, vol. 107, p. 102344, 2023.

[7] K. Artiouchine, P. Baptiste, and C. Dürr, "Runway sequencing with holding patterns," *European Journal of Operational Research*, vol. 189, no. 3, pp. 1254–1266, 2008.

[8] Y. Hong, B. Choi, S. Lee, K. Lee, and Y. Kim, "Optimal and practical aircraft sequencing and scheduling for point merge system," *IFAC-PapersOnLine*, vol. 50, no. 1, pp. 14 644–14 649, 2017.

[9] H. Balakrishnan and B. Chandran, "Scheduling aircraft landings under constrained position shifting," in *AIAA guidance, navigation, and control conference and exhibit*, 2006, p. 6320.

[10] D. Bertsekas, *Dynamic programming and optimal control*. Athena scientific, 2005, vol. 1.

[11] "FlightRadar24: Tokyo Haneda International Airport (Available online)," https://www.flightradar24.com/data/airports/hnd/arrivals.

APPENDIX

A. Derivation for Δt_{m+1} using equations of motion

We derive (10a) and (12a) using equations of motion.

In the DEC maneuver with a speed decrements, the aircraft decelerates for a period of $(a\Delta V)/B$ and then travels rest of the distance until the next segment at a constant speed $V_{\text{next}} = V_{\text{current}} - a\Delta V$ where $V_{\text{current}} = V_0 - \vartheta_m \Delta V$. The distance travelled during deceleration is

$$D_{\text{dec}} = \frac{(V_{\text{next}}^2 - V_{\text{current}}^2)}{2(-B)} = \frac{(a\Delta V)(V_{\text{next}} + V_{\text{current}})}{2B}. \tag{40}$$

For D_{gap} in (11), the distance remaining after deceleration is

$$D_{\text{rem}} = D_{\text{gap}} - D_{\text{dec}} = \frac{2BD_{\text{gap}} - (a\Delta V)(V_{\text{next}} + V_{\text{current}})}{2B}. \tag{41}$$

The relative time at the next segment is

$$\begin{aligned}
\Delta t^+ &= \Delta t + \text{Time to decelerate} + \text{Time to next segment} && (42)\\
&= \Delta t + \frac{a\Delta V}{B} + \frac{D_{\text{rem}}}{V_{\text{next}}} && (43)\\
&= \Delta t + \frac{a\Delta V}{B} + \frac{2BD_{\text{gap}} - (a\Delta V)(V_{\text{next}} + V_{\text{current}})}{2BV_{\text{next}}} && (44)\\
&= \Delta t + \frac{2BD_{\text{gap}} + 2(a\Delta V)V_{\text{next}} - (a\Delta V)(V_{\text{next}} + V_{\text{current}})}{2BV_{\text{next}}} && (45)\\
&= \Delta t + \frac{2BD_{\text{gap}} + (a\Delta V)(V_{\text{next}} - V_{\text{current}})}{2BV_{\text{next}}} && (46)\\
&= \Delta t + \frac{2BD_{\text{gap}} - (a\Delta V)^2}{2BV_{\text{next}}}. && (47)
\end{aligned}$$

On the other hand, for the HOLD and PMS maneuvers, the action a increments Δt by aT_{hold} and aT_{pms} respectively.